Heliyon 11 (2025) e41948

Contents lists available at ScienceDirect

Heliyon

journal homepage: www.cell.com/heliyon

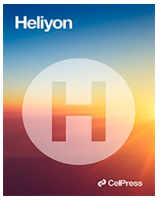

Research article

Reciprocal regulation between DNMT3A/3B and microRNAs miRs-299-3p/-30e is a causal factor for the downregulation of microRNAs targeting androgen receptor in prostate cancer

Kavya Ganapathy [a], Christian F. Harrs [a], Samuel Harris [a], Stephen J. Staklinski [a], Ayman Khatib [a], Jong Y. Park [b], Ratna Chakrabarti [a,*]

[a] Burnett School of Biomedical Sciences, University of Central Florida, Orlando, FL, USA
[b] Moffitt Cancer Center, Tampa, FL, USA

ARTICLE INFO

Keywords:
MicroRNA
Promoter methylation
DNMT
Prostate cancer disparity

ABSTRACT

Background: Promoter hypermethylation is one of the events that downregulate microRNAs (miRNA), resulting in the differential expression of genes implicated in the progression of cancer. We previously reported that microRNAs (miRNA)-299-3p and −30e target androgen receptor (AR) and are downregulated in advanced prostate cancer (PCa). Here we report that miR-34c, an AR targeting miRNA and miR-299-3p, both are differentially downregulated in PCa cells from African American (AA) and Caucasian American (CA) patients due to disparate promoter hypermethylation in these miRNA genes.

Methods: We performed bisulfite sequencing based promoter methylation analysis with or without treatment with DNA methyl transferase (DNMT) inhibitor 5-Aza-2′-deoxycytidine (AzaC). Luciferase reporter assays and RNA pulldown assays are conducted for miRNA -DNMT interaction analysis. We performed DNMT activity assays and ectopic expression of miRNAs to study their effects.

Results: We observed higher promoter methylation of these miRNA genes in cells derived from an AA patient compared to cells of CA origin, which can be reversed through AzaC treatment. Differential expression and activity of DNMT3A and 3B are noted in PCa cells from AA and CA origins. Immunoprecipitation of Ago revealed bound DNMT3A and 3B mRNAs with miRs-299-3p and −30e in the RISC. Luciferase reporter assays confirmed binding of miRs-299-3p and −30e to the UTRs of DNMT3A and 3B mRNAs. Overexpression of miRs-299-3p and −30e downregulated DNMT3A/B mRNA and protein expression and DNMT activity of DNMTs. Ectopic expression of miR-299-3p restored expression of miRs-34c and −30e in PCa cells. Similarly, overexpression of miR-30e restored expression of miRs-34c and -299-3p.

Conclusion: Our study provides evidence that ectopic expression of miRs-30e and -299-3p restore the loss of expression of miRs-299-3p and −34c miRNAs mediated by DNMT-induced promoter hypermethylation. This study establishes a feedback regulation between AR targeting miRNAs and DNMTs in PCa cells and provides an insight into the mechanism of the aberrant expression of AR in advanced PCa that is potentially mediated through the downregulation of miRs-299-3p, −34c and −30e and stabilization of expression and activities of DNMTs.

* Corresponding author. 12722 Research Parkway, Orlando, FL, 32826, USA.
E-mail address: ratna.chakrabarti@ucf.edu (R. Chakrabarti).

https://doi.org/10.1016/j.heliyon.2025.e41948
Received 17 May 2024; Received in revised form 9 January 2025; Accepted 13 January 2025
Available online 23 January 2025

Abbreviations

AA	African American
ADT	Androgen deprivation therapy
AR	Androgen receptor
AzaC	5-Aza-2′-deoxycytidine
CA	Caucasian American
CRPC	Castration-resistant prostate cancer
DNMT	DNA methyl transferases
FFPE	Formalin fixed paraffin embedded
miRNA	MicroRNA
PCa	Prostate cancer
RISC	RNA-induced silencing complex
RLU	Relative Luciferase Units
RNA-IP	RNA immunoprecipitation
snRNA	Small nuclear RNAs
UTR	Untranslated region

1. Introduction

Epigenetic mechanisms that significantly influence gene expression through transcription regulation, play crucial roles in aberrant expression of oncogenes and tumor suppressor genes implicated in cancer progression. DNA methylation through deposition of a methyl group at the cytosines of CpG dinucleotides that are over-represented in the gene promoters [1], can silence transcription of tumor suppressor genes [2]. In humans, CpG site methylation is mediated by three canonical DNMTs, DNMT1, DNMT3A and DNMT3B [3], of which DNMT1 is involved in methylation maintenance [4], while DNMT3A and DNMT3B are involved in de novo methylation [5]. Although tightly regulated in healthy tissues, aberrant expression and activity of DNMTs emerge in cancerous tissues through their mutations, overexpression, and/or phosphorylations [6–8]. Overexpression of DNMTs is noted to be associated with PCa that exhibits resistance to the FDA-approved AR antagonist drug enzalutamide [9]. Inhibition of DNA methylation and DNMT silencing showed improved sensitivity of PCa to enzalutamide [9].

Prostate cancer (PCa) claims a significant number of lives in men in the Western world [10]. As prostate tumor cells rely on androgens functioning through AR for growth, blocking of the AR signaling pathway through androgen deprivation therapy (ADT) and inhibition of AR functions through enzalutamide became the mainstay of therapy for aggressive and metastatic PCa [11,12]. Although initially effective, resistance to enzalutamide occurs, and eventually leads to the development of castration-resistant prostate cancer (CRPC) [12]. CRPC often results in metastasis and shorter patient survival [13]. The mechanisms of genetic and epigenetic alterations leading to the development of CRPC have been explored extensively which indicates that AR gene amplification, and mutations in AR along with its cofactors are responsible for aberrant transcriptional activities [14–16]. Epigenetic reprogramming is also activated during metastatic progression of PCa [17]. Importantly, differential methylation of gene promoters was noted in AA PCa patients compared to CA patents where AA PCa patients exhibit a positive correlation with increased DNA methylation and tumor aggressiveness [18].

Silencing of miRNAs through promoter hypermethylation of miRNA host gene is a common event in PCa progression [19]. MiRNAs are regulatory molecules that cause gene silencing through translational repression and destabilization of specific mRNAs [20]. Aberrant expression of miRNAs is frequently noted during tumorigenesis and metastatic progression of various cancers including PCa [20, 21]. Studies have shown a negative correlation between androgen-dependent AR function and DNMT expression. Prolonged treatment with AR antagonists and ADT triggers increased DNMT activities and appearance of a splice variant of AR, which facilitates the development of drug-resistant and highly aggressive PCa [21]. It has been shown that the promoter of miR-375 is hypermethylated in AR-negative PCa cells, whereas the miR-375 promoter is almost unmethylated in AR-positive PCa cells [22]. miR-498 expression is negatively correlated with radio-resistance of esophageal cancer and increases radiosensitivity through inhibition of DNMT3B expression [23].

MicroRNAs have been shown to regulate the epigenome through modification of DNA methylation by targeting DNA methyltransferases. miR-20a-5p targets DNMT3B and inhibits promoter methylation of retinol-binding protein in ovarian cancer [24]. miR-143 exerts its tumor suppressor functions and promotes cisplatin sensitivity of ovarian cancer cells through inhibition of DNMT3A [25].

We previously reported a reduced expression of three AR targeting miRNAs miRs-34c, 299-3p and −30e in advanced PCa compared to uninvolved prostate tissues, specifically in tumors from AA patients compared to the CA patients [26–28]. Using cell culture and xenograft models, we demonstrated the tumor suppressor roles of miRs-299-3p and −30e in PCa through primarily targeting AR. In this study, we show that differential promoter hypermethylation of AR-targeting miRNA genes is a contributing factor for the reduced expression of these miRNAs in AA and CA tumor cells. We also provide evidence that these miRNAs are involved in regulating DNMT3A and DNMT3B expression and themselves are regulated through a negative feedback loop.

2. Materials and methods

2.1. Patient tissues acquisition

Prostate clinical samples were procured from the CHTN (Cooperative Human Tissue Network, Southern division) at the University of Alabama at Birmingham (UAB) under the protocol approved by the Internal Review Board. Prostate tissues, obtained from radical prostatectomies, were evaluated by a pathologist and the formalin fixed paraffin embedded (FFPE) tissue sections were used for macro-dissection of tumor and uninvolved areas. RNA from the tissue samples was extracted and used for quantitative real-time PCR (qRT-PCR).

2.2. Quantitative real-time PCR

Total RNA from tissue samples and cells were extracted, used for cDNA synthesis, and qRT-PCR using our published protocols [26,28]. A mirNome miRNA profiling kit (System Biosciences) for tissue samples and miScript RT II Kit (Qiagen) for cell lines were used for cDNA synthesis. Subsequent qRT-PCR was conducted using specific primers for miR-34e-5p, miR-299-3p and miR-30e and 3 small nuclear RNAs (U6 snRNA, RNU43 snoRNA, RNU1A snRNA) (System Biosciences) as internal controls, and 2X Maxima SYBR Green/ROX qPCR Master Mix (Thermo Fisher Scientific). For qRT-PCR of mRNAs, specific primers for the target mRNAs and EIF3D and RPL13a internal controls (10X QuantiTect primers, Qiagen) and QuantiTect SYBR PCR Kit (Qiagen) were used. The QuantStudio 7 thermal cycler (Applied Biosystems) was used for qRT-PCR. The raw CT values were normalized with the reference genes to obtain $^{\Delta}$CT values and the relative expression of miRNAs and mRNAs between tumor and uninvolved tissues or experimental and control cells was analyzed using $^{\Delta\Delta}$CT method.

2.3. Cell lines and transfection

F-12 HAM Kaighn's modification media (Sigma Aldrich) media were used for maintaining MDA-PCa-2b (RRID: CVCL_4748, ATCC) and PC-3 (RRID: CVCL0035, ATCC) cells. DMEM (Sigma Aldrich) were used for maintaining LNCaP-104S cells (RRID: CVCL_M126, a gift from Dr. Shutsung Liao from University of Chicago); RPMI-1640 base media (Sigma Aldrich) was used for maintaining C4-2B (RRID: CVCL4784 a gift from Dr. Leland Chung, Cedars-Sinai Medical Center) and 22Rv-1 cells (RRID: CVCL_1045, ATCC). All base media were supplemented with 10 % heat-inactivated or non-heat-inactivated (MDA-PCa-2b) Fetal Bovine serum (FBS) (Atlanta Biologicals), 1 % antibiotic-antimycotic (Thermo Fisher Scientific), 1 % L-glutamine (Thermo Fisher Scientific). For MDA-PCa-2b cells, 25 ng/mL cholera toxin, 10 ng/mL mouse EGF, 0.005 mM phosphoethanolamine, 100 pg/mL hydrocortisone, 45 nM sodium selenite and 0.005 mg/mL human recombinant insulin (Thermo Fisher Scientific) were used as additives. LNCaP-104S cells were maintained in complete media containing 1 nM dihydrotestosterone (Sigma Aldrich). All cell lines were authenticated within last 3 years by short tandem repeat profiling, and mycoplasma contamination was tested by DAPI staining of all cells to confirm mycoplasma-free status of the cells. Stable sublines of C4-2B and 22Rv-1 cells were generated as we described earlier [26,27]. For all experiments, stable cell lines with or without doxycycline (1 μg/mL) induction were used.

2.4. Promoter methylation analysis

Genomic DNA from LNCaP-104S and MDA-PCa-2b cells were extracted using QIAamp DNA Mini Kit (Qiagen) as per the kit protocol. The integrity of the extracted DNA was evaluated using agarose gel electrophoresis. Genomic DNA samples from LNCaP-104S and MDA-PCa-2b cells were used for bisulfite conversion using the EpiTect Fast Bisulfite Conversion Kit (Qiagen) as per manufacturer's protocol. Bisulfite converted DNAs were quantified using a nanodrop-1000 spectrophotometer and used for PCR amplification using specific primers for the promoter regions of miRs-34c and −299 genes. Specific primer sequences are shown below:

miR-299 CpG Location 1: F: 5′-TTTGTGTGGTATTTGGAGAG-3′,
R: 5′-AATCAAAATCTCCTCCCC A-3'
miR-299 CpG Location 2: F: 5′TTAAATTAAGTTTTGTTTTGGGAAA-3'
R:5′ATCCCACATACATATTCAAAATATATATAA-3'
miR-34c CpG Location 1: F: 5′-GAATGAGGGAGTGGAGGAG-3'
R: 5′-ATACCAAACCTCCCCTTC C-3'
miR-34c CpG Location 2: F: 5′GTTTGGTATTTTTGGGGGTTA-3'
R: 5′-ACCACAATACAATCAACTAATAACACTAC-3'
miR-34c CpG Location 3: F: 5′-AGGTAGTGTTATTAGTTGATTGTATTGTG-3'
R: 5′-CCTCCAAAAATTTTACTTTCCTAAC-3'

GoTaq Green HotStart master-mix (2X) (Promega) was used for PCR amplification, and the amplified products were analyzed in agarose gels (NuSieve AGAROSE 3:1 Lonza 3:1). The specific bands were gel-extracted using the QIAquick Gel Extraction Kit (Qiagen) as per manufacturer protocol. Gel extracted PCR amplified products were ligated into the pGEMT-Easy vector (Promega). Plasmid DNA was extracted using PureYield Plasmid Miniprep Kit (Promega) and the cloned inserts were verified in agarose gels. Plasmid DNAs from at least five colonies for each sample were analyzed by DNA sequencing and the sequences were analyzed to identify the percentage of methylation of each individual CpG site across the selected colonies as well as the total percent methylation per CpG location for each individual colony.

2.5. 5′-azacytidine treatment

Promoter methylation experiments were conducted using genomic DNAs from LNCaP-104S and MDA-PCa-2b treated with 5-Aza-2′-deoxycytidine (AzaC) (Selleckchem). Cells were grown to 70 % confluency and treated with DMSO or AzaC for 5 days with daily change in media containing DMSO or AzaC. Cells were harvested for genomic DNA extraction, bisulfite conversion, PCR amplification, cloning of the amplified products and sequence analysis.

2.6. Luciferase reporter assays

The binding sites of miR-299-3p and miR-30e on the 3′UTRs of the target mRNAs (DNMT3A and DNMT3B) were determined by *in-silico* analysis and amplified from the genomic DNA extracted from PCa cell lines. Amplified products were sequence verified and cloned into pmirGLO Dual-Luciferase vector (Promega) at the NheI and SalI sites downstream of the firefly luciferase gene. For site-directed mutagenesis, a 3-base pair mutation was introduced at the 3′ end of the miRNA recognition site using the PCR based quick-change mutagenesis method. Site-directed mutagenesis primers (SDM primers) were designed to contain 16-24 base pairs homologous complementary regions at the 5′ end followed by 8-base pairs homologous complementary regions at the 3′ end. PCR amplified products were Dpn1 (New England Biolab) digested and used for transformation of *E. coli*. Plasmid DNAs were extracted, and the mutant inserts were sequence verified. The wild type or the mutated constructs were used for Dual Luciferase reporter assays. 22Rv-1-299 stable line and C4-2B-30e stable lines were seeded in 24-well dishes and transfected after 24hrs with either control luciferase reporter plasmids containing no 3′UTR inserts, experimental wild-type luciferase reporter plasmids or experimental mutated luciferase reporter plasmids. Twenty-four hours after transfection, cells were induced with doxycycline and incubated for an additional 48hrs. Next, cells were lysed and activities of the Firefly and Renilla luciferases were measured using the Dual-Glo Luciferase kit (Promega) as per manufacturer's protocol. The luminescence from the firefly and Renilla luciferase was quantified using a plate-reader (Synergy Neo2 Plate Reader, BioTek). The luminescence in RLU was background corrected and normalized to get a ratio for control and experimental samples. Next, luciferase expression was calculated as the normalized ratio of experimental sample divided by the normalized ratio of control sample and plotted as a percentage.

2.7. RNA immunoprecipitation

Argonaut-2-based immunoprecipitation was performed for miR-299-3p expressing C4-2B cells using the EZ-Magna-RIP Kit (EMD Millipore) according to the manufacturer's protocol and our published methods [26]. For each immunoprecipitation reaction, doxycycline induced or uninduced C4-2B-299 cells were harvested at 48 h post induction and lysed in RNA-IP lysis buffer. Lysates were incubated with Anti-Pan Ago mouse monoclonal antibodies or mouse IgG negative control antibodies conjugated magnetic beads (EMD Millipore). Phenol-chloroform extraction followed by ethanol precipitation were used for extraction of the precipitated RNAs. The precipitated RNA and the input RNA were used for cDNA synthesis and qRT-PCR for quantification of miR-299-3p. Biotinylated miR-30e Mimic (Qiagen) was used to precipitate DNMT3A and DNMT3B using RNA-IP assays. 22RV-1 cells were transfected with either negative control biotinylated mimics or biotinylated miR-30e mimic using RNAiMax following transfection conditions as per manufacturer's protocol. After 48 h of transfection, cells were harvested, and miRNA-mRNA complexes were precipitated using streptavidin magnetic beads (Sigma Aldrich). Bead bound total RNA was isolated using phenol-chloroform extraction and ethanol precipitation. Input RNAs and the precipitated RNAs were used for cDNA synthesis and qRT-PCR for miR-30e-5p and DNMT3A and DNMT3B. The Ct values of the precipitated RNAs were normalized to the Ct values of the input samples and used to calculate the percent precipitation of the target mRNAs.

2.8. Western Blotting

Total proteins were extracted from the induced and uninduced stable C4-2B and 22Rv-1 sublines and used for SDS-PAGE followed by Western Blotting. Cells were harvested 48h post-induction and lysed using RIPA lysis buffer supplemented with protease and phosphatase inhibitors (Fisher Scientific). Fifty micrograms of total proteins were separated on a Bis-Tris gel and transferred to PVDF membranes. Transfer membranes were probed with primary antibodies specific for DNMT3A (Mouse monoclonal Santa Cruz) and DNMT3B (Rabbit polyclonal, ProteinTech) followed by goat anti-mouse or anti-rabbit secondary antibodies (Pierce). Alpha-Tubulin antibodies (Cell Signaling) were used as the internal controls. Positive signals were visualized upon reaction with ECL Chem-iluminescence substrate (BioRad) and imaged using a ChemiDoc MP Imaging System (BioRad). Comparative expression of DNMTs was determined based on densitometry analysis of the polypeptide band intensities normalized to internal controls using ImageJ software.

2.9. DNMT activation assay

The overall DNMT activity (de novo as well as maintenance DNA methyltransferases) in parental cells and transfected sublines was measured using the EpiQuik DNA Methyltransferase Activity/Inhibition Assay Kit (Epigentek), as per manufacturer's protocol. Parental cells or transfected cells with or without induction were grown to ~80 % confluency and nuclear proteins were extracted using the EpiQuik Nuclear Extraction Kit (Epigentek) as per manufacturer's protocol. Ten microgram nuclear extracts were bound to the microtiter plates and after washing off unbound proteins, capture antibodies for DNMTs followed by detection antibodies were added to the wells. After washing the unbound antibodies, developer solution was added to the wells and incubated for 3.5hrs. The

change in color of the solution was detected as a measure of DNMT activities in a spectrophotometer at 450 and 655 nm, and the background corrected values were processed by first subtracting the OD at 655 nm from OD at 450 nm. This background corrected values were used to calculate the DNMT activity using the following formula:

$$DNMT\ Activity\ (OD\ /\ hour\ /\ mg) = \frac{\left(\text{Sample OD}_{\text{background corrected}} - \text{Blank OD}_{\text{background corrected}}\right)}{(\text{protein } \mu g^{*} \text{ x hours}^{**})}$$

* Corresponds to the amounts of nuclear proteins used in the assay in μg.** Corresponds to the initial incubation time in hours after addition of the samples/blank.

2.10. Statistical analysis

All statistical analyses were performed using Student's *t*-test or one-way ANOVA for independent measures using GraphPad Prism. The statistical significance was set at $p < 0.05$. Data was represented as mean ± SD.

3. Results

3.1. Differential expression and promoter methylation of miR-299 and miR-34c genes in prostate cancer

We examined the expression of miRs-34c-5p and -299-3p in total RNA extracted from macro-dissected prostate tumors and adjacent uninvolved tissues from AA and CA PCa patients. The patient inclusion criteria are PSA, Gleason score, surgical margins, lymph node invasion, extracapsular extension, and seminal vesicle invasion as we reported previously [28]. A comparative analysis of the fold change in expression between tumors and matched uninvolved tissues from different racial group of patients demonstrated a trend in downregulation of miRs-34c-5p and -299-3p in AA patients, whereas a broader distribution of CA patients could be noted who exhibit relatively higher expression levels. A 2.4- and 3.6-fold difference in the average expression of miR-299-3p and miR-34c-5p,

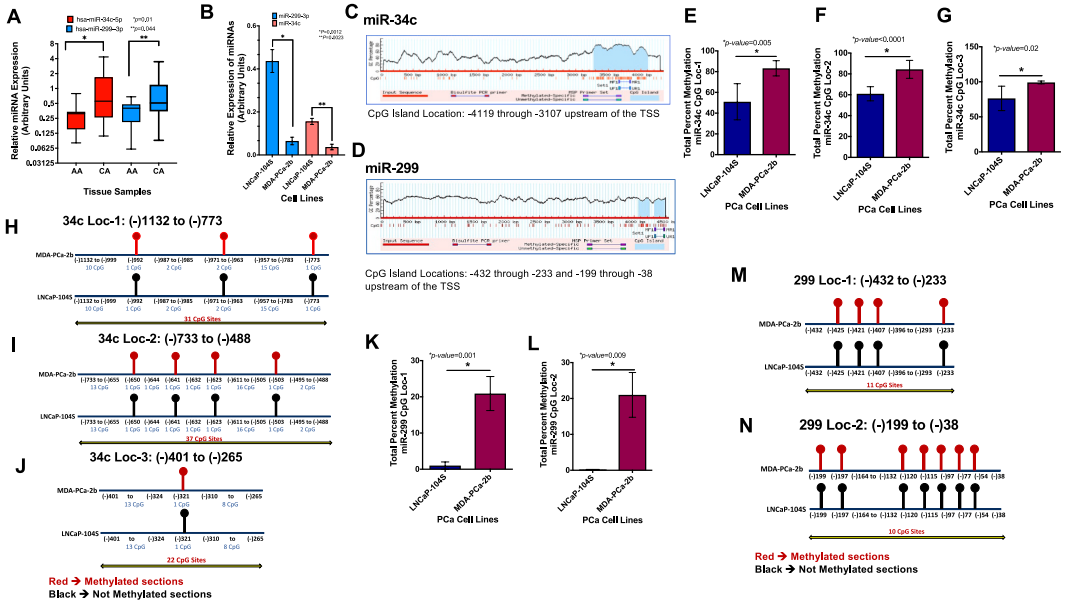

Fig. 1. Differential expression and promoter methylation of *miR-34c* and-*299-3p* genes in AA and CA PCa. **A**: Average fold change in expression of miRs-34c and -299-3p in PCa tissues showed a significant down regulation of these miRNAs in tumors from the AA (n = 10) patients compared to the CA patients (n = 12) **B**: qRT-PCR analysis of the expression of miRs-299-3p and −34c showed reduced expression of these miRNAs in MDa-PCa-2b cells compared to the LNCaP-104S cells. Data show the average ± SD of three biological replicates. **C** and **D**: Location of the CpG islands at the *miR-34c* and-*299* gene promoters as predicted by the MethPrimer prediction tool. TSS: transcription start site. **E**–**G**: Bisulfite sequencing analysis showed a significant increase in the total methylation of the *miR-34c* promoter CpG sites in location 1 (**E**), location 2 (**F**), and location 3 (**G**) in MDA-PCa-2b cells compared to the LNCaP-104S PCa cells. **H**–**J**: Ball and Stick models for the *miR-34c* promoter CpG sites location 1 (H), location 2 (**I**), and location 3 (**J**) showed Differentially Methylated Regions (DMRs) between MDA-PCa-2b and LNCaP-104S cells. Red color indicates the methylated sites in the MDA-PCa-2b cells which were not methylated in the LNCaP-104S cells as shown in black. **K** and **L**: Bisulfite sequencing analysis exhibited a significant increase in the total methylation of the *miR-299* promoter CpG sites in location 1 (**K**) and location 2 (**L**) in MDA-PCa-2b cells compared to the LNCaP-104S PCa cells. **M** and **N**: Ball and Stick models for the *miR-299* promoter CpG sites Location 1 (**M**) and location 2 (**N**) showed DMRs between MDA-PCa-2b and LNCaP-104S cells. Red color indicates the methylated sites in the MDA-PCa-2b cells which were not methylated in the LNCaP-104S as shown in black.

respectively were noted between AA and CA tumors (Fig. 1A).

Differential expression of these miRNAs in PCa cell lines from AA (MDA-PCa-2b) and CA (LNCaP-104S) origins were observed. Noticeably lower levels of miRs-34c-5p (6.6-fold) and -299-3p 9.2-fold) were noted in MDA-PCa-2b cells compared to LNCaP-104S cells (Fig. 1B). As previous studies confirm epigenetic regulation as a causal factor for downregulation of miRNA expression in cancer [29,30], these observations led us to investigate the promoter methylation status of *miR-299* and *miR-34c* genes in MDA-PCa-2b and LNCaP-104S cell lines. We used MethPrimer tool [31] to predict the CpG islands within ~4000 bp upstream sequences from the first base of *miR-34c* and *miR-299* genes. Our analysis showed the presence of one large CpG island spanning from −1132 bp to −265 bp for *miR-34c* promoter, which we analyzed separately as 3 CpG Locations (CpG Location 1: 1132 bp to −773 bp; CpG Location 2: 733 bp to −488 bp; CpG Location 3: 401 bp to −265 bp), and two CpG locations for *miR-299* promoter (CpG Location 1: 432 bp to −233 bp; CpG Location 2: 199 bp to −38 bp), for miR-299 (Fig. 1C and D).

Bisulfite conversion followed by sequence analysis revealed an overall increase in total promoter methylation for the CpG locations 1, 2 and 3 for *miR-34c* promoter in the MDA-PCa-2b cells (34c-CpG Loc-1: 83 %; 34c-CpG Loc-2: 84 %; 34c-CpG Loc-3: 99 %) compared to the LNCaP-104S cells (34c-CpG Loc-1: 51 %; 34c-CpG Loc-2: 61 %; 34c-CpG Loc-3: 76 %) (Fig. 1E, F and G). Furthermore, differentially methylated sites (DMEs) were identified for the CpG locations 1, 2 and 3 in *miR-34c* promoter. These CpG sites were found to be methylated only in MDA-PCa-2b cells, but not in LNCaP-104S cells (Fig. 1H, I and J). Bisulfite sequence analysis for *miR-299* promoter methylation also showed an overall increase in total promoter methylation for the CpG locations 1 and 2 for *miR-299* gene in the MDA-PCa-2b cells (299-CpG Loc-1: 20 %; 299-CpG Loc-2: 21 %) compared to the LNCaP-104S cells (299-CpG Loc-1: 1 %; 299-CpG Loc-2: no methylation) (Fig. 1K and L). Specific DMEs for CpG Locations 1 and 2 in miR-299 also showed methylation only in MDA-PCa-2b cells but not in LNCaP-104S cells (Fig. 1M and N). These data demonstrated that miR-34c and miR-299 are differentially downregulated of in AA compared to CA PCa, and that these miRNA genes exhibited differential promoter hypermethylation in the AA MDA-PCa-2b compared to the CA LNCaP-104S PCa cells and that these miRNAs.

3.2. Inhibition of DNMT activity restored expression of miR-34c and miR-299-3p and reduced promoter methylation

We used DNA methyltransferase (DNMT) inhibitor AzaC to investigate the effect of inhibition of DNMTs on promoter methylation

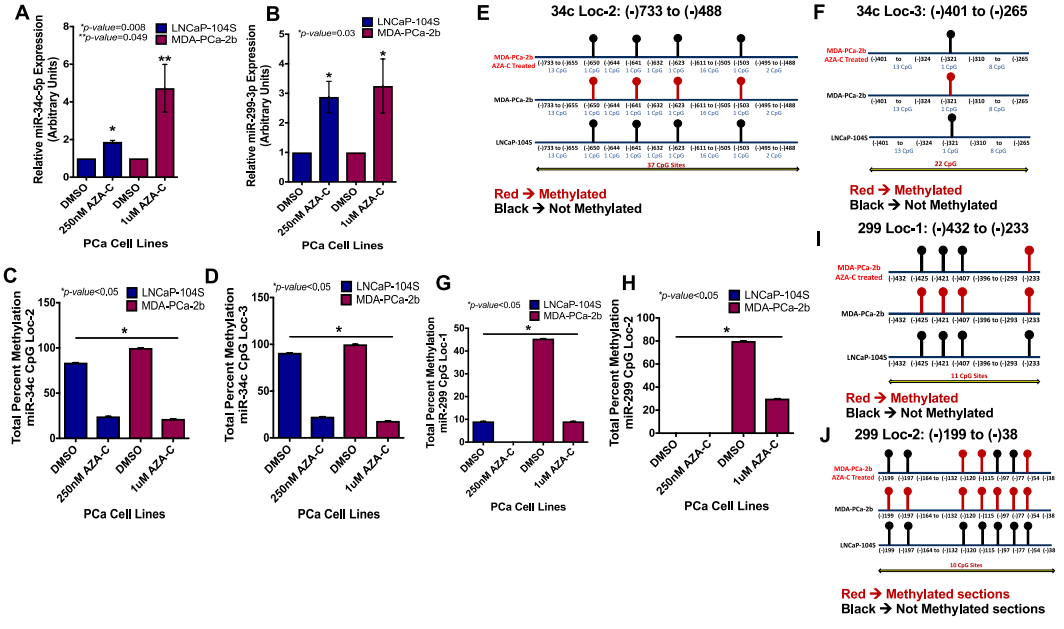

Fig. 2. Treatment with AzaC restored expression of miRNAs and reverted promoter methylation. **A** and **B**: qRT-PCR analysis exhibited increased expression of miR-34c (**A**) and miR-299-3p (**B**) in LNCaP-104S and MDA-PCa-2b cells upon treatment with AzaC compared to DMSO treatments. Data show the mean ± SD of 3 independent experiments. **C** and **D**: Bisulfite sequencing analysis showed a significant reduction in the total methylation of the *miR-34c* promoter CpG sites in location 2 (**C**) and in location 3 (**D**) in MDA-PCa-2b and in LNCaP-104S cells upon treatment with AzaC compared to the respective DMSO controls. Data show the mean ± SD of at least 5 colonies/cell line. **E** and **F**: Ball and Stick models for the *miR-34c* promoter CpG sites location 2 (**E**), and location 3 (**F**) upon AzaC treatment showed 100 % reversal of DMRs in MDA-PCa-2b cells, which are unmethylated in LNCaP-104S cells. Red color indicates the methylated sites in the MDA-PCa-2b cells, whereas black indicates unmethylated sites. Data show the mean ± SD of at least 5 colonies/location. **G** and **H**: Bisulfite sequencing analysis showed a significant reduction in the total methylation of the *miR-299* promoter CpG sites in location 2 (**G**) and in location 3 (**H**) in MDA-PCa-2b and LNCaP-104S cells upon treatment with AzaC compared to the respective DMSO controls. Data show the mean ± SD of the sequencing data from at least 5 colonies. **I** and **J**: Ball and Stick models for the *miR-299* promoter CpG sites in location 1 (**I**), and in location 2 (**J**) upon AzaC treatment showed demethylation of the 3 out of 4 sites (loc-1) and 4 out of 7 sites (loc 2) in DMRs in MDA-PCa-2b cells, which are unmethylated in the LNCaP-104S cells.

of miRNA genes. We observed that for both miRNA gene promoters, treatment with 250 nM of AzaC restored expression of miR-34c and miR-299-3p in LNCaP-104S cells (1.9-fold and 2.9-fold, respectively) compared to the control (DMSO treatment) (Fig. 2A). The dose and the time of treatment of AzaC was empirically determined to obtain optimum restoration based on the doses and times used in a previously published study [32]. MDA-PCa-2b cells, on the other hand required a higher dose of AzaC (1 μM) to restore expression of miRs-34c and -299-3p (4.7-fold and 3.2-fold, respectively) when compared to the control (Fig. 2B). The dose and the time of treatment for this cell line was optimized using published information [33]. Bisulfite sequence analysis of the promoter methylation upon AzaC treatment showed a decrease in total methylation in the CpG sites in miR-34c gene (Loc-2: 100 %–22 %; Loc-3: 100 %–18 %) in MDA-PCa-2b cells when compared to the DMSO treated cells (Fig. 2C and D). A similar decrease in promoter methylation for miR-34c gene in the CpG sites in locations 2 and 3 in LNCaP-104S cells treated with AzaC (Loc-2: 84 %–24 %; Loc-3: 91 %–23 %) was noted when compared to DMSO treated cells. A reversal of methylation in the differentially methylated CpG sites for miR-34c gene in Loc-2 and Loc-3 was noted in MDA-PCa-2b cells treated with AzaC when compared to the DMSO treated cells (Fig. 2E and F). No changes were observed for the Loc-1 CpG sites. (Supplemental Fig. 1). Similarly, there was an overall decrease in methylation in the CpG sites for miR-299 gene in MDA-PCa-2b cells (Loc-1: 45 %–9 %; Loc-2: 80 %–30 %) treated with AzaC when compared to the DMSO treated cells and in LNCaP-104S cells (Loc-1: 9 %–0 %) compared to DMSO treated cells (Fig. 2G and H). A 50%–75 % reversal of methylation in the differentially methylated CpG sites for miR-299 gene in Loc-1 (75 %) and Loc-2 (50 %) was noted in MDA-PCa-2b cells treated with AzaC when compared to the DMSO treated cells (Fig. 2I and J). A higher decrease in total methylation in the CpG locations for miR-299 gene in the MDA-PCa-2b cells was noted when compared to the LNCaP-104S cells (Fig. 2G and H). In summary, these observations confirms that −299 and miR-34c gene promoters are differentially methylated in PCa cells from AA and CA origins by DNMTs and can be reversed upon inhibition of DNMTs.

3.3. Differential expression and activities of DNMTs in prostate cancer cells

Next, we intended to monitor the expression and activity of DNMTs in AA and CA cell lines as our previous results confirmed differential methylation of *miR-299* and *miR-34c* promoters in MDA-PCa-2b and LNCaP-104S cells. Although DNMT3A and DNMT3B are the enzymes responsible for de novo methylation and are often involved in cancer progression [34,35], we also monitored the expression and activity of DNMT1, the enzyme responsible for maintenance methylation, as its role in cancer progression has been documented in multiple studies [36,37]. Quantitative RT-PCR analysis revealed differential endogenous expression pattern of *DNMT1*, *DNMT3A* and *DNMT3B* mRNAs in different PCa cell lines, C4-2B, 22Rv-1, LNCaP-104S and PC-3 from CA origin and MDA-PCa-2b from AA origin (Fig. 3A, B and C). We noted that *DNMT1* and *DNMT3B* but not *DNMT3A* mRNAs showed a higher expression in the AA cell line (MDA-PCa-2b) compared to the CA cell lines. We next examined the activity of DNMTs in the nuclear protein extracts from MDA-PCa-2b and LNCaP-104S cells using an ELISA-based colorimetric activity assay, which measured overall activities from all three DNMTs. Our results showed an increased DNMT activity in the MDA-PCa-2b cells compared to the LNCaP-104S cells (Fig. 3D), which aligns with our observation of higher promoter methylation of miRNA genes and increased requirement of AzaC to restore expression of miRs-299-3p and −34c in these cells.

3.4. Regulation of DNMT3A and DNMT3B expression by AR targeting miRNAs

Apart from being regulated by epigenetic modifications, miRNAs themselves can directly target and regulate epigenetic modulators such as DNMTs and histone modifiers [38]. In this regard, we intended to identify whether the AR-targeting miRNAs also target any of the DNMTs such as DNMT1, DNMT3A and DNMT3B in PCa. *In silico* analysis of the target prediction databases (miRDB, TargetScan) suggested that both *DNMT3A* and *DNMT3B* have binding sites at their 3′UTRs of miR-299-3p and miR-30e, another AR-targeting miRNA (Fig. 4A). We previously reported the miR-30e functions as a tumor suppressor miRNA [26] and exhibited significant downregulation in PCa tumors, specifically in AA tumors compared to CA tumors [28]. In this study, we examined the regulation of

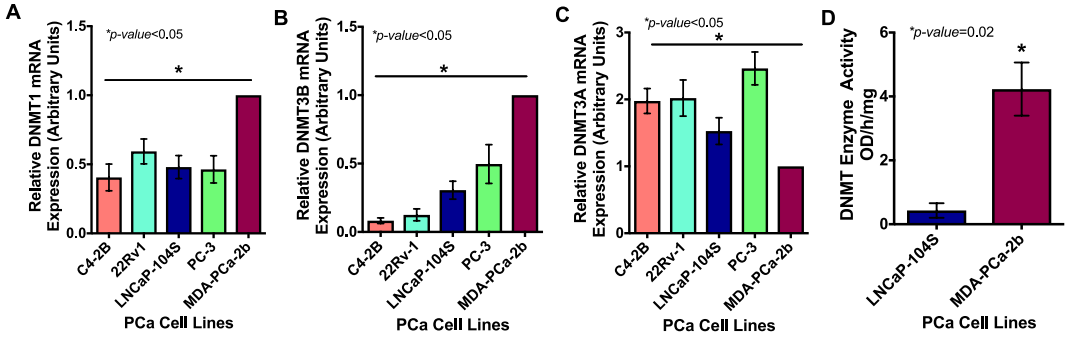

Fig. 3. Differential expression and activities of DNMTs in PCa cells. A and **B**: qRT-PCR analysis showed lower DNMT1 (**A**) and DNMT3B (**B**) mRNA expression in all CA PCa cells compared to the AA MDA-PCa-2b PCa cells. **C**: qRT-PCR analysis showed higher DNMT3A mRNA expression in all CA PCa compared to the AA cells. **D**: ELISA-based DNMT activity assay showed an overall higher DNMT activity in MDA-PCa-2b cells compared to the LNCaP-104S cells.

expression of DNMT3A and DNMT3B by direct targeting of miR-299-3p and miR-30e. Induced 22Rv-1-299 cells were transiently transfected with the luciferase reporter constructs containing the 3′UTRs of DNMT3A and DNMT3B with wild type or mutated binding sites for miR-299-3p. Our results showed decreased luciferase activities for both *DNMT3A* (46 %) and *DNMT3B* (48 %) mRNAs for the construct with the wild type binding sites, which was not noted in the mutated constructs. The control luciferase reporter construct did not show any alterations in the luciferase activity (Fig. 4B and C). For the reporter assay for miR-30e targeting of *DNMT3A* and *DNMT3B* mRNAs, doxycycline induced C4-2B-30e cells were used. Luciferase reporter assays using constructs containing the wild type and mutated binding sites for miR-30e at the 3′UTR of DNMT3A and DNMT3B were performed using induced C4-2B-30e cells. Reduced luciferase activity was noted in transfected cells for both DNMT3A (53 %) and DNMT3B (50 %) wild type 3-UTR containing constructs, but not upon mutation of the single binding site in DNMT3A and double binding sites in DNMT3B UTRs. The control luciferase reporter construct showed no decrease in luciferase activity upon transfection into the induced C4-2B-30e cells (Fig. 4D and E). These results confirm destabilization of DNMT3A and DNMT3b mRNAs by miRs-299-3p and −30e.

3.5. Interaction of DNMT3A and DNMT3B with miR-299-3p and miR-30e

To confirm the direct interactions between miR-299-3p and DNMT mRNAs, RNA immunoprecipitation was conducted using Argonaut (Ago)-2-antibodies using C4-2B-299 cells with or without induction with doxycycline. Our results from qRT-PCR analysis showed significant enrichment of *DNMT3A* (1.9-fold) and *DNMT3B* (1.6- fold) mRNAs in the Ago-2 antibody mediated precipitated RISCs from the induced C4-2B-299 cells compared to uninduced controls. No enrichment of DNMT mRNAs was noted when nonspecific control IgG was used (Fig. 4F). Additionally, qRT-PCR analysis of the input RNA showed decreased *DNMT3A* and *DNMT3B* mRNA expressions (38 % and 55 %) in the induced C4-2B-299 cells compared to uninduced controls (Fig. 4G). We previously reported an enrichment of miR-299-3p (3.2-fold) in the Ago-2 antibody mediated precipitated RISCs from the induced C4-2B-299 cells compared to the uninduced controls and an increased expression of miR-299-3p in the input samples from the induced C4-2B-299 cells [27]. Next, 22Rv-1 cells were used to study direct interactions between the miR-30e and *DNMT3A* and *DNMT3B* mRNAs. We used biotinylated miR-30e mimic or negative control mimic for transient transfection of 22Rv-1 PCa cells. Precipitation of RNA complexes with streptavidin beads and qRT-PCR analysis of the precipitated RNA showed enrichment of *DNMT3A* and *DNMT3B* mRNAs (6.5 % and 5

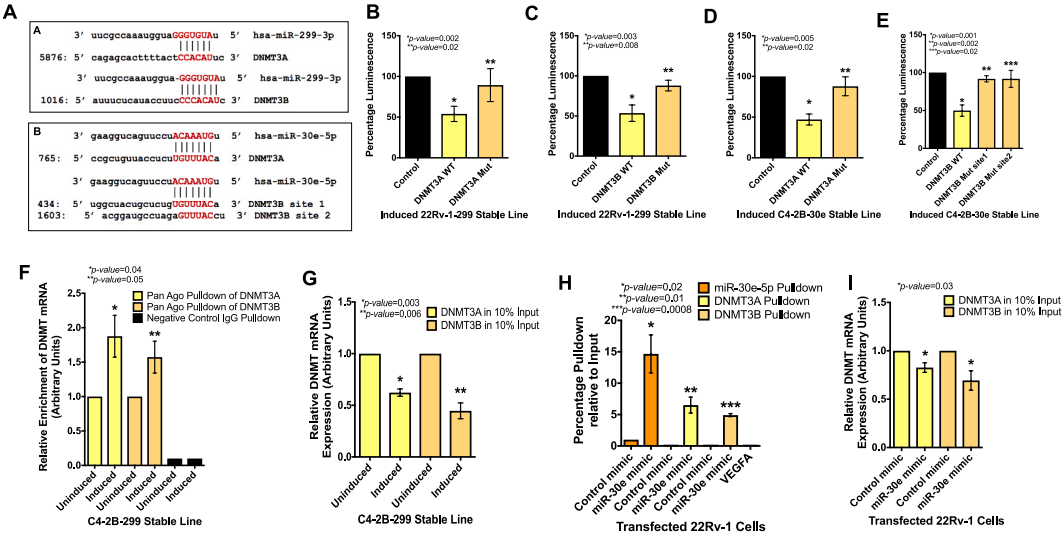

Fig. 4. MicroRNAs miRs-299-3p and -30e interact with DNMTs in PCa cells. **A**: Sequence of the binding sites of miRs-299-3p (A) and −30e (B) at the 3′UTRs of *DNMT3A* and *DNMT3B* mRNAs as predicted by the TargetScan database search. Two binding sites were predicted for miR-30e on the 3′UTR of *DNMT3B* mRNA (B). **B** and **C**: Luciferase reporter assays showed binding of miR-299-3p to the specified seed sequences at the 3′UTR of *DNMT3A* (B) and *DNMT3B* (C) mRNAs as observed by the decreased luciferase activity upon transfection with the construct containing the wild-type (WT) but not with the mutated (Mut) 3′UTRs of *DNMT3A* (B), and *DNMT3B* (C). Data show the mean ± SD of three independent experiments **D** and **E**. Luciferase reporter assays showed binding of miR-30e to the specified seed sequences at the 3′UTR of *DNMT3A* (**D**) and *DNMT3B* (**E**) mRNAs as observed by the decreased luciferase activity upon transfection with the construct containing the wild-type (WT) but not with the mutated (Mut) 3′UTRs of *DNMT3A* (**D**) and *DNMT3B* (both sites) (**E**). Data show the mean ± SD of three independent experiments. **F**: qRT-PCR analysis of the pan-Ago2 antibody-based RNA-IP experiment showed enrichment of *DNMT3A* and *DNMT3B* mRNAs in the RISC of the induced C4-2B-299 cells compared to the uninduced controls. **G**: qRT-PCR analysis of the 10 % input RNA showed decreased expression of *DNMT3A* and *DNMT3B* mRNAs in the induced C4-2B-299 cells line compared to the uninduced controls. Data show the mean ± SD of three biological replicates. **H**: qRT-PCR analysis of the biotinylated mimic-mediated RNA precipitation showing enrichment of miR-30e, *DNMT3A* and *DNMT3B* mRNAs relative to input samples in the 22Rv-1 cells upon transfection of biotinylated miR-30e mimic compared to the control mimic. *VEGFA* mRNA was used as a negative control, which showed no precipitation with biotinylated miR-30e mimic nor the control mimic. **I**: qRT-PCR analysis of the 10 % input samples showed an increased expression of miR-30e and decreased expressions of *DNMT3A* and *DNMT3B* mRNAs in 22Rv-1 cells transfected with biotinylated miR-30e mimic. Data show the mean ± SD of three biological replicates.

%, respectively) in the cells transfected with biotinylated miR-30e mimic but not in the cells transfected with negative control mimic (Fig. 4H). In our previous report, we confirmed precipitation of miR-30e in cells transfected with biotinylated miR-30e, which was not noted for the negative control mimic [26]. To rule out the possibility of nonspecific interactions, we monitored expression of VEGFA which was not a target of miR-30e. No precipitation of *VEGFA* mRNA in the cells transfected with either miR-30e mimic or control mimic was noted confirming the specificity of the RNAIP experiments (Fig. 4H). qRT-PCR analysis of the input RNA samples showed decreased expression of *DNMT3A* and *DNMT3B* mRNAs (*DNMT3A*: 17 %; *DNMT3B*: 30 %) in cells transfected with miR-30e mimic compared to the negative control mimic (Fig. 4I). We previously reported an increased expression of miR-30e in 22Rv-1 cells transfected with miR-30e mimic [26]. These observations confirm the interaction of miRs-299-3p and −30e with *DNMT3A* and *DNMT3b* mRNAs in a complex.

3.6. Expression of miR-299-3p and miR-30e reduced expression and activities of DNMTs

Our results confirmed direct interactions between miRs-299-3p and −30e with *DNMT3A* and *DNMT3B* mRNAs, which led us to study the effect of overexpression of miR-299-3p and miR-30e on *DNMT3A* and *DNMT3B* mRNA and protein expression, and enzymatic activity. C4-2B-299 and 22Rv-1-299 cells with or without induction were used for expression analysis using qRT-PCR. Our results showed decreased mRNA levels for both *DNMT3A* and *DNMT3B* (16 % and 38 %, respectively) in the induced C4-2B-299 and 22Rv-1-299 cells (*DNMT3A*: 26 % and *DNMT3B* 24 %) compared to the uninduced controls (Fig. 5A and B). We previously reported a tumor suppressor function of miR-299-3p in xenograft tumors of C4-2B-299 cells [27]. Expression of miR-299-3p reduced tumor growth prolonged survival and decreased AR and Ki67 in tumor tissues. To corroborate the *in vitro* effects of miR-299-3p on DNMT to *in vivo* results, we examined the expression of *DNMT3A* and *DNMT3B* mRNAs in mice tumors expressing miR-299-3p. qRT-PCR analysis showed significant downregulation of these DNMT mRNAs in tumors expressing miR-299-3p induced with the feed containing

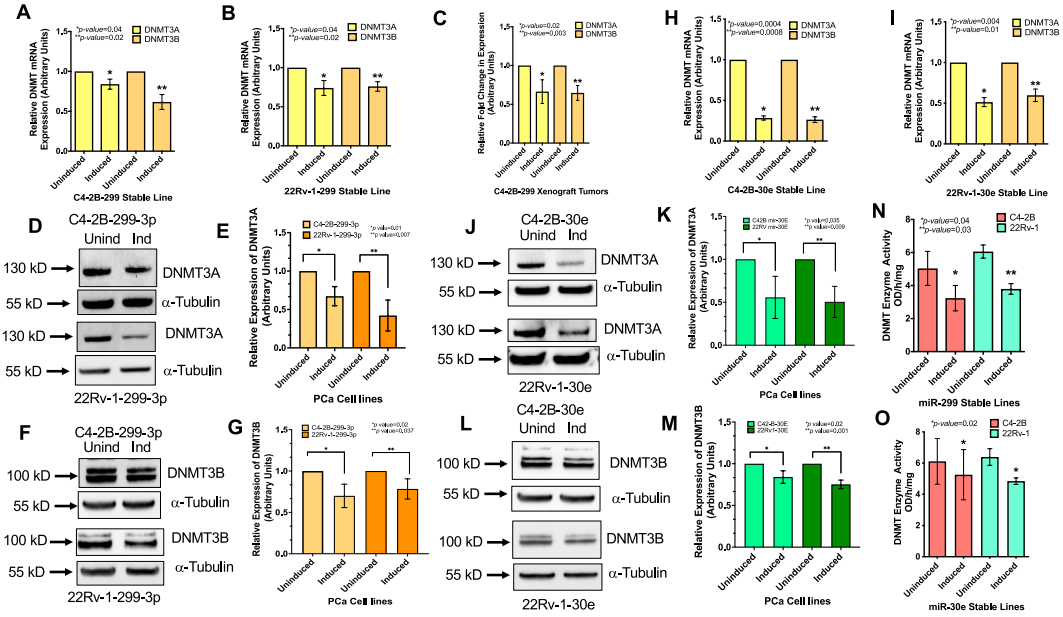

Fig. 5. Expression of miRs-299-3p and -30e downregulated expression and activities of DNMT3A and DNMT3B. A–C: qRT-PCR analysis showed decreased expression of DNMT3A and DNMT3B mRNAs in the induced C4-2B-299 (**A**) and 22Rv-1-299 (**B**) cells and in the xenograft tumors of C4-2B-299 (**C**) compared to the uninduced control cells and tumors. **D** and **E**: Western blot (**D**) and densitometric (**E**) analysis showed a reduced expression of DNMT3A in the induced C4-2B-299 (upper two panels) and 22Rv-1-299 (lower two panels) cells compared to the uninduced cells. Alpha-tubulin was used as the loading control. Data show the mean ± SD of 3 independent experiments. **F** and **G**: Western blot (**F**) and densitometric (**G**) analysis showed a reduced expression of DNMT3B in the induced C4-2B-299 (upper two panels) and 22Rv-1-299 (lower two panels) cells compared to the uninduced cells. Alpha-tubulin was used as the loading control. Data show the mean ± SD of 3 independent experiments. **H** and **I**: qRT-PCR analysis showed reduced expression of DNMT3A and DNMT3B mRNAs in the induced C4-2B-30e (**H**) and 22Rv-1-30e (**I**) cells compared to the uninduced control cells. Data show the mean ± SD of 3 independent experiments. **J** and **K**: Western blot (**J**) and densitometric (**K**) analysis showed a reduced expression of DNMT3A in the induced C4-2B-30e (upper two panels) and 22Rv-1-30e (lower two panels) cells compared to the uninduced cells. Alpha-tubulin was used as the loading control. Data show the mean ± SD of 3 biological replicates. **L** and **M**: Western blot (**L**) and densitometric (**M**) analysis showed a reduced expression of DNMT3B in the induced C4-2B-30e (upper two panels) and 22Rv-1-30e (lower two panels) cells compared to the uninduced cells. Alpha-tubulin was used as the loading control. Data show the mean ± SD of 3 biological replicates. As the figure has several panels, all Western blots are presented as cropped images. Full blots are presented in the Supplementary information file. **N** and **O**: DNMT activity assays showed an overall decreased activity upon miRs-299-3p and −30e expression in the induced C4-2B-299 and 22Rv-1-299 (**N**), and in the C4-2B-30e and 22Rv-1-30e (O) cells compared to the respective uninduced controls. Data show the mean ± SD of 3 biological replicates.

doxycycline (dox-feed) compared to tumors from mice given regular feed (Fig. 5C). Western blot analysis showed significant down-regulation of DNMT3A and DNMT3B in the induced C4-2B-299 (33 % and 30 %, respectively) and 22Rv-1 cells (58 % and 22 %, respectively) compared to the uninduced controls (Fig. 5D, E, F and G). To study the effect of miR-30e restoration, both induced C4-2B-30e and 22Rv-1-30e cells were used for expression analysis of DNMT mRNAs and proteins. Our analysis showed decreased expressions of both *DNMT3A* and *DNMT3B* (70 % and 74 %, respectively) mRNAs in induced C4-2B-30e cells and 22Rv-1-30e cells (49 % and 40 %, respectively) compared to the uninduced controls (Fig. 5H and I). Western blot analysis showed downregulation of DNMT3A and DNMT3B in the induced C4-2B-30e (44 % and 16 %, respectively) and 22Rv-1-30e cells (50 % and 25 %, respectively) compared to the uninduced controls (Fig. 5J, K, L and M). A comparative analysis of the results showed an average of 1.25-fold upregulation of miRs-30e and −34c-5p, and an average of 0.36-fold reduction in DNMT3A and DNT3B expression in cells with the restored expression of miR-299-3p. The relative changes in miRNAs and DNMTs can be calculated as a net upregulation of miRNAs by 1.6-fold compared to the levels of DNMTs. Similarly, an average of 2.7-fold upregulation of miRs-299-3p and 34c, and 0.59-fold reduction in DNMTs were noted in cells expressing miR-30e. These changes show a net upregulation of miRNAs by 3.3-fold compared to the levels of DNMTs. Hower these estimation does not reflect the actual effects as the binding stoichimetry and miRNA turnover can influence the efficacy of destabilization of mRNAs by miRNAs.

Next, we determined DNMT activities using ELISA since promoter methylation is dependent on the activity of DNMTs in these cells. The assays showed a significant decrease in the overall DNMT activities in the induced C4-2B-299 cells (36 %) and 22Rv-1-299 cells (38 %) compared to the uninduced controls (Fig. 5N). DNMT activity assays also showed a significant decrease in the overall DNMT activities in induced C4-2B-30e cells (13 %) and 22Rv-1-30e cells (25 %) compared to the uninduced controls (Fig. 5O). Taken together, these studies confirmed that both miR-299-3p and miR-30e regulate expression and activities of DNMT3A and DNMT3B.

3.7. Expression of DNMT-targeting miRNAs increased expression of miRNAs that showed loss of expression in prostate cancer cells

From our results, it is evident that miR-299-3p and miR-34c-5p are directly regulated through promoter methylation by DNMTs and in turn, miR-299-3p and miR-30e directly target and regulate DNMT3A and DNMT3B activities. To test the rescue effect of miRNAs on the expression of other miRNAs that are methylated, we studied the effect of overexpression of miR-299-3p on the expression of miR-34c-5p and miR-30e. We used two PCa cell lines overexpressing miR-299-3p (C4-2B-299 and 22Rv-1-299) for expression analysis of these miRNAs by qRT-PCR. Our analysis showed that increased expression of miR-299-3p in the induced C4-2B-299 cells restored expression of miR-30e (1.2-fold) as well as miR-34c-5p (1.3-fold) compared to the uninduced control cells (Fig. 6A). Similar effects were noted in the induced 22Rv-1-299 cells, which showed that increased expression of miR-299-3p restored expression of miR-30e (2.3-fold) and miR-34c (3-fold) compared to the uninduced control (Fig. 6B). We next examined the effect of overexpression of miR-30e on the expression of miR-34c-5p and miR-299-3p. We used cell lines overexpressing miR-30e (C4-2B-30e and 22Rv-1-30e) for expression analysis of these miRNAs by qRT-PCR. Our analysis showed that increased expression of miR-30e in the induced C4-2B-30e cells partially restored expression of miR-299-3p (1.1-fold) as well as miR-34c (1.4-fold) compared to the uninduced control (Fig. 6C). qRT-PCR analysis also showed that increased expression of miR-30e in the induced 22Rv-1-30e cells showed rescue effects on expression of miR-299-3p (1.6-fold) and miR-34c (1.8-fold) compared to the uninduced control (Fig. 6D). These results confirmed that increased expression of miRs-299-3p or −30e override the loss of expression of miR-299-2p and miR-34c miRNAs mediated by DNMT induced promoter methylation.

4. Discussion

In this study, we showed promoter hypermethylation of miRs-34c and −299 miRNA genes in various PCa cells, including the cells of AA origin. miR-34c, a member of the miR-34 family, showed a negative correlation with the expression of AR in PCa tumors, and has

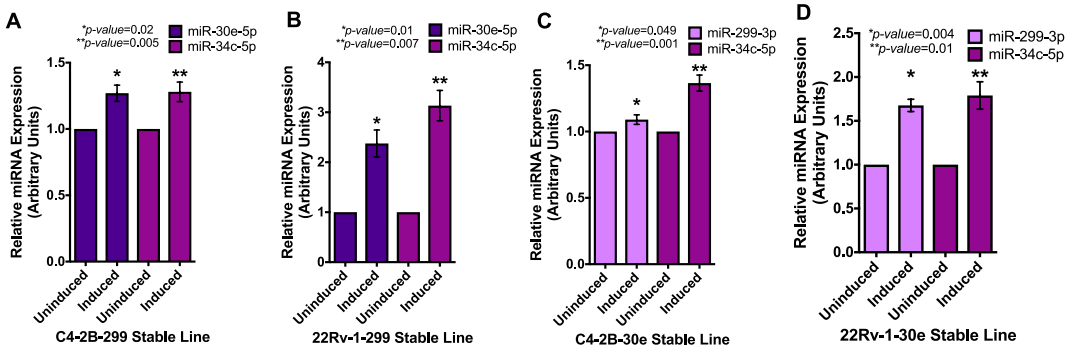

Fig. 6. Expression of miR-299-3p and -30e restored expression of downregulated miRNAs in PCa cells. **A** and **B**: qRT-PCR analysis showed increased expression of miR-30e and miR-34c-5p in the induced C4-2B-299 cells (**A**) and 22Rv-1-299 (**B**) cells compared to the uninduced controls. Data show the mean ± SD of 3 independent experiments. **C** and **D**. qRT-PCR analysis showed increased expression of miR-299-3p and miR-34c-5p in the induced C4-2B-30e cells (**C**) and 22Rv-1-30e (**D**) cells compared to the uninduced controls. Data show the mean ± SD of 3 independent experiments.

a binding site in the 3′UTR of the AR and exhibited a direct interaction with AR mRNAs [39]. It has been noted that epigenetic regulatory mechanisms often govern the expression of intergenic miRNAs in cancer. Therefore, intergenic miRNAs, miRs-299 and -34c, may be regulated by the same mechanism. Downregulation of miRs-34c and its family member −34b in various cancers has already shown significant correlation with CpG island hypermethylation [40]. However, our study provides the first demonstration of a higher percentage of total number of methylated CpGs and a distinctly different pattern of CpG sites methylated in the *miR-34c* gene promoter in cell lines derived from racially disparate PCa patients. In support of our observation, a previous study reported differential downregulation of miR-34b in AA tumors compared to CA tumors, and confirmed promoter hypermethylation of *miR-34b* gene as the causal factor for its downregulation in PCa [41]. We also showed a racially disparate pattern of CpG island methylation in the *miR-299* gene promoter in PCa cell lines. Regarding expression of miR-299, several studies reported the DNA hypermethylation of miRNA genes on 14q32.31 which also contains the *miR-299* gene [30,42–44]. Our study is the first to demonstrate that promoter methylation is a contributing factor of downregulated expression of miR-299-3p in PCa. We also noted AzaC treatment-based reversal of promoter methylation and restored expression of miRs-299 and miR-34c in both AA and CA PCa cell lines.

We also reported differential expression and activities of the DNMTs (DNMT1, DNMT3A and DNMT3B) which are frequently overexpressed in multiple cancers [45]. We showed increased expression of DNMT1 and DNMT3B in the AA PCa cells compared to CA cells, which corroborated with our observations of increased total miRs-299 and miR-34c promoter methylation in AA compared to CA PCa cells. Taken together, our results demonstrated that aberrant promoter methylation of *miR-299* and *miR-34c* by DNMTs is responsible, in part, for their downregulation in PCa, where differential methylation of specific CPG sites and overall promoter hypermethylation affect racially disparate expression.

It has been known that DNMTs are aberrantly expressed in cancer cells and modulate the expression of coding and noncoding genes through epigenetic regulations. While miRNAs are regulated by DNMTs, miRNAs themselves can also regulate DNMTs directly or indirectly, thereby offering a powerful tool to reverse the malignant behavior of cancer cells through modulation of the epigenetic machinery [45]. Previous studies have reported that DNMT3A and DNMT3B are the direct targets of miRs-101, -143, −152, −148a and −29 in several cancer types [46–51]. In this study, results based on luciferase reporter assays, RNA-IP and ELISA-based activity assays collectively showed that miR-299-3p and miR-30e directly target and regulate DNMT3A and DNMT3B mRNA expression and modulate DNMT activities, which may alter the epigenetic landscape to exert an overall tumor suppressor function. In summary, we identified miR-299-3p and miR-30e to be epigenetic miRNAs (epi-miRNAs) as upstream regulators of the DNA methylation epigenetic machinery with the potential to reverse aberrant methylation patterns that contribute to gene silencing in PCa.

The complex functional relationship between miRNAs and the epigenetic machinery is a key feature in understanding and manipulating gene expression profiles that contribute to tumorigenesis. Specifically in cancer, several studies have explored miRNA regulation by DNMTs such as miR-29b-DNMT3A/3B in ovarian cancer [52], miR-200b-DNMT3A in breast cancer [53], miR-143-DNMT3A in colorectal cancer [46], miR-152-DNMT1 in cholangiocarcinoma [54], miR-148/152-DNMT1 in breast cancer [51] and miR-145-DNMT3A in ovarian cancer [55]. Our study exhibited a miRNA-DNMT feedback loop that maintains a balance of expression of miR-299-3p and miR-34c and DNMTs. The aberrant functioning of DNMTs can disrupt the balance and result in loss of expression of these miRNAs in PCa. Our observation also revealed a possibility that restored expression of these miRNAs can have a rescue effect on the expression of other tumor suppressor miRNAs that directly undergo DNMT-mediated promoter methylation in PCa. Our results from miR-299-3p expression in PCa cells showed not only reduced expression and activities of DNMTs by miR-299-3p but also restored expression of miR-30e and miR-34c-5p. Along this line, DNA methylation has also been implicated in the downregulation of miR-30 family members [56,57]. Hence, it can be speculated that restored expression of miR-30e upon overexpression of miR-299-3p is an effect of miR-299-3p mediated dampening of DNMT activities. This effect was noted in both androgen-sensitive C4-2B and androgen-insensitive 22Rv-1 PCa cells, which shows that restoration of miRs-299-3p and −30e is effective in PCa cells

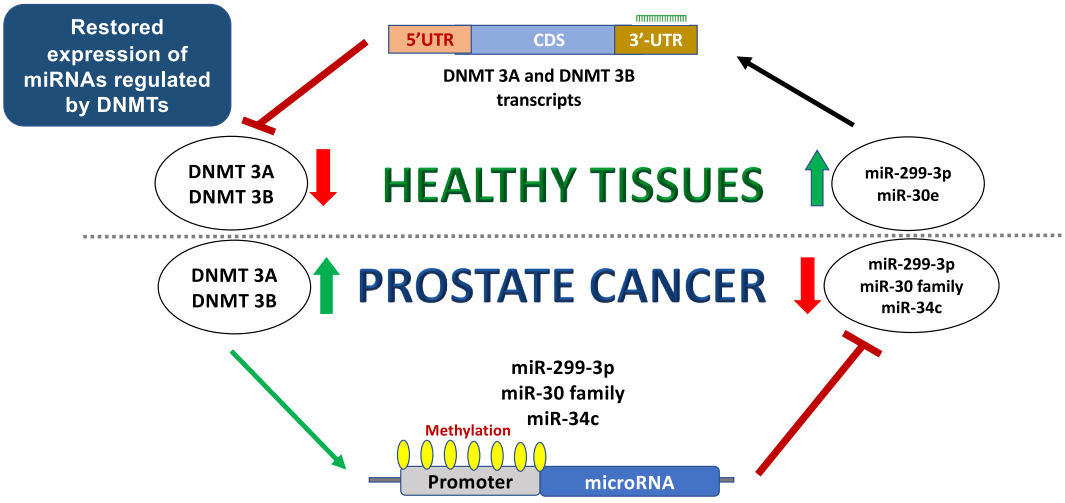

Fig. 7. miRNA-DNMT feedback loop in PCa progression.

irrespective of the androgen sensitivity status.

5. Conclusion

We demonstrated the involvement of a miRNA-DNMT regulatory loop in PCa progression (Fig. 7). We hypothesized that there is an increased expression of the tumor suppressor miRNAs, such as miR-299-3p, miR-30e and miR-34c-5p, in the normal tissues. Of these miRNAs, miR-299-3p and miR-30e directly target and downregulate the expression of DNMT3A and DNMT3B, and overall DNMT activity, to maintain the epigenetic modulators under control. However, in PCa, high expression of DNMT3A and DNMT3B [58] can downregulate the expression of miR-299-3p and miR-34c-5p through promoter hypermethylation as seen in this study. This collective downregulation of the tumor suppressor AR-targeting miRNAs due to promoter hypermethylation could result in PCa progression. It has been documented that enzalutamide resistant PCa cells express DNMT at a higher concentration and targeting DNMTs improve enzalutamide sensitivity of PCa cells [9]. This is a major disadvantage of enzalutamide treatment as reduced AR function may promote DNMT activities and AR-independent PCa progression. Because miR-299-3p and −30e target both AR and DNMTs, restored expression of these miRNAs may avoid, or delay the development of enzalutamide resistance mediated by increased DNMT expression and promoter methylation leading to biochemical recurrence of PCa.

CRediT authorship contribution statement

Kavya Ganapathy: Writing – original draft, Validation, Methodology, Data curation, Conceptualization. **Christian F. Harrs:** Validation, Methodology, Data curation. **Samuel Harris:** Validation, Data curation, Conceptualization. **Stephen J. Staklinski:** Validation, Data curation. **Ayman Khatib:** Validation, Data curation. **Jong Y. Park:** Writing – review & editing, Validation, Conceptualization. **Ratna Chakrabarti:** Writing – review & editing, Writing – original draft, Supervision, Resources, Methodology, Funding acquisition, Formal analysis, Conceptualization.

Consent for publication

N/A.

Ethics approval and consent to participate

The study was conducted in accordance with the Declaration of Helsinki and approved by the Institutional Review Board Committee of University of Central Florida (SBE-14-10298). This study did not require ethics approval as only deidentified clinical samples were used. Samples were collected at the CHTN (Cooperative Human Tissue Network, Southern division) at the University of Alabama at Birmingham) under the protocol approved by the Internal Review Board. At UAB, all patients have written informed consents to be enrolled in the study.

Availability of data and materials

Experimental and clinical data are available upon request to Dr. Ratna Chakrabarti (ratna.chakrabarti@ucf.edu).

AI technologies

No AI technologies were used for preparingthe manuscript.

Funding

This research was funded by grants from the Department of Defense Prostate Cancer Research Program (PCRP) (Grant/Award Number: W81XWH-11-1-0563) and National Institutes of Health (Grant/Award Number: R21CA226611) to R.C.

Declaration of competing interest

The authors declare that they have no known competing financial interests or personal relationships that could have appeared to influence the work reported in this paper.

Acknowledgements

We thank the support of Dr William E. Grizzle for the prostate tissues from Cooperative Human Tissue Network at the University of Alabama in Birmingham.

Appendix A. Supplementary data

Supplementary data to this article can be found online at https://doi.org/10.1016/j.heliyon.2025.e41948.

References

[1] S. Saxonov, P. Berg, D.L. Brutlag, A genome-wide analysis of CpG dinucleotides in the human genome distinguishes two distinct classes of promoters, Proc. Natl. Acad. Sci. U.S.A. 103 (2006) 1412–1417.
[2] A. Bird, DNA methylation patterns and epigenetic memory, Genes Dev. 16 (2002) 6–21.
[3] F. Lyko, The DNA methyltransferase family: a versatile toolkit for epigenetic regulation, Nat. Rev. Genet. 19 (2018) 81–92.
[4] A. Hermann, R. Goyal, A. Jeltsch, The Dnmt1 DNA-(cytosine-C5)-methyltransferase methylates DNA processively with high preference for hemimethylated target sites, J. Biol. Chem. 279 (2004) 48350–48359.
[5] T. Chen, Y. Ueda, J.E. Dodge, Z. Wang, E. Li, Establishment and maintenance of genomic methylation patterns in mouse embryonic stem cells by Dnmt3a and Dnmt3b, Mol. Cell Biol. 23 (2003) 5594–5605.
[6] R. Deplus, L. Blanchon, A. Rajavelu, A. Boukaba, M. Defrance, J. Luciani, F. Rothe, S. Dedeurwaerder, H. Denis, A.B. Brinkman, F. Simmer, F. Muller, B. Bertin, M. Berdasco, P. Putmans, E. Calonne, D.W. Litchfield, Y. de Launoit, T.P. Jurkowski, H.G. Stunnenberg, C. Bock, C. Sotiriou, M.F. Fraga, M. Esteller, A. Jeltsch, F. Fuks, Regulation of DNA methylation patterns by CK2-mediated phosphorylation of Dnmt3a, Cell Rep. 8 (2014) 743–753.
[7] T.J. Ley, L. Ding, M.J. Walter, M.D. McLellan, T. Lamprecht, D.E. Larson, C. Kandoth, J.E. Payton, J. Baty, J. Welch, C.C. Harris, C.F. Lichti, R.R. Townsend, R. S. Fulton, D.J. Dooling, D.C. Koboldt, H. Schmidt, Q. Zhang, J.R. Osborne, L. Lin, M. O'Laughlin, J.F. McMichael, K.D. Delehaunty, S.D. McGrath, L.A. Fulton, V. J. Magrini, T.L. Vickery, J. Hundal, L.L. Cook, J.J. Conyers, G.W. Swift, J.P. Reed, P.A. Alldredge, T. Wylie, J. Walker, J. Kalicki, M.A. Watson, S. Heath, W. D. Shannon, N. Varghese, R. Nagarajan, P. Westervelt, M.H. Tomasson, D.C. Link, T.A. Graubert, J.F. DiPersio, E.R. Mardis, R.K. Wilson, DNMT3A mutations in acute myeloid leukemia, N. Engl. J. Med. 363 (2010) 2424–2433.
[8] S.R. Morey Kinney, D.J. Smiraglia, S.R. James, M.T. Moser, B.A. Foster, A.R. Karpf, Stage-specific alterations of DNA methyltransferase expression, DNA hypermethylation, and DNA hypomethylation during prostate cancer progression in the transgenic adenocarcinoma of mouse prostate model, Mol. Cancer Res. 6 (2008) 1365–1374.
[9] E. Farah, Z. Zhang, S.M. Utturkar, J. Liu, T.L. Ratliff, X. Liu, Targeting DNMTs to overcome enzalutamide resistance in prostate cancer, Mol. Cancer Therapeut. 21 (2022) 193–205.
[10] R.L. Siegel, A.N. Giaquinto, A. Jemal, Cancer statistics, 2024, CA A Cancer J. Clin. 74 (2024) 12–49.
[11] C. Tran, S. Ouk, N.J. Clegg, Y. Chen, P.A. Watson, V. Arora, J. Wongvipat, P.M. Smith-Jones, D. Yoo, A. Kwon, T. Wasielewska, D. Welsbie, C.D. Chen, C. S. Higano, T.M. Beer, D.T. Hung, H.I. Scher, M.E. Jung, C.L. Sawyers, Development of a second-generation antiandrogen for treatment of advanced prostate cancer, Science 324 (2009) 787–790.
[12] M. Tucci, C. Zichi, C. Buttigliero, F. Vignani, G.V. Scagliotti, M. Di Maio, Enzalutamide-resistant castration-resistant prostate cancer: challenges and solutions, OncoTargets Ther. 11 (2018) 7353–7368.
[13] N.L. Sharma, C.E. Massie, A. Ramos-Montoya, V. Zecchini, H.E. Scott, A.D. Lamb, S. MacArthur, R. Stark, A.Y. Warren, I.G. Mills, D.E. Neal, The androgen receptor induces a distinct transcriptional program in castration-resistant prostate cancer in man, Cancer Cell 23 (2013) 35–47.
[14] W. Abida, J. Cyrta, G. Heller, D. Prandi, J. Armenia, I. Coleman, M. Cieslik, M. Benelli, D. Robinson, E.M. Van Allen, A. Sboner, T. Fedrizzi, J.M. Mosquera, B. D. Robinson, N. De Sarkar, L.P. Kunju, S. Tomlins, Y.M. Wu, D. Nava Rodrigues, M. Loda, A. Gopalan, V.E. Reuter, C.C. Pritchard, J. Mateo, D. Bianchini, S. Miranda, S. Carreira, P. Rescigno, J. Filipenko, J. Vinson, R.B. Montgomery, H. Beltran, E.I. Heath, H.I. Scher, P.W. Kantoff, M.E. Taplin, N. Schultz, J. S. deBono, F. Demichelis, P.S. Nelson, M.A. Rubin, A.M. Chinnaiyan, C.L. Sawyers, Genomic correlates of clinical outcome in advanced prostate cancer, Proc. Natl. Acad. Sci. U.S.A. 116 (2019) 11428–11436.
[15] B. De Laere, P.J. van Dam, T. Whitington, M. Mayrhofer, E.H. Diaz, G. Van den Eynden, J. Vandebroek, J. Del-Favero, S. Van Laere, L. Dirix, H. Gronberg, J. Lindberg, Comprehensive profiling of the androgen receptor in liquid biopsies from castration-resistant prostate cancer reveals novel intra-AR structural variation and splice variant expression patterns, Eur. Urol. 72 (2017) 192–200.
[16] D.A. Quigley, H.X. Dang, S.G. Zhao, P. Lloyd, R. Aggarwal, J.J. Alumkal, A. Foye, V. Kothari, M.D. Perry, A.M. Bailey, D. Playdle, T.J. Barnard, L. Zhang, J. Zhang, J.F. Youngren, M.P. Cieslik, A. Parolia, T.M. Beer, G. Thomas, K.N. Chi, M. Gleave, N.A. Lack, A. Zoubeidi, R.E. Reiter, M.B. Rettig, O. Witte, C.J. Ryan, L. Fong, W. Kim, T. Friedlander, J. Chou, H. Li, R. Das, H. Li, R. Moussavi-Baygi, H. Goodarzi, L.A. Gilbert, P.N. Lara Jr., C.P. Evans, T.C. Goldstein, J.M. Stuart, S.A. Tomlins, D.E. Spratt, R.K. Cheetham, D.T. Cheng, K. Farh, J.S. Gehring, J. Hakenberg, A. Liao, P.G. Febbo, J. Shon, B. Sickler, S. Batzoglou, K.E. Knudsen, H. H. He, J. Huang, A.W. Wyatt, S.M. Dehm, A. Ashworth, A.M. Chinnaiyan, C.A. Maher, E.J. Small, F.Y. Feng, Genomic hallmarks and structural variation in metastatic prostate cancer, Cell 175 (2018) 889.
[17] M.M. Pomerantz, X. Qiu, Y. Zhu, D.Y. Takeda, W. Pan, S.C. Baca, A. Gusev, K.D. Korthauer, T.M. Severson, G. Ha, S.R. Viswanathan, J.H. Seo, H.M. Nguyen, B. Zhang, B. Pasaniuc, C. Giambartolomei, S.A. Alaiwi, C.A. Bell, E.P. O'Connor, M.S. Chabot, D.R. Stillman, R. Lis, A. Font-Tello, L. Li, P. Cejas, A.M. Bergman, J. Sanders, H.G. van der Poel, S.A. Gayther, K. Lawrenson, M.A.S. Fonseca, J. Reddy, R.I. Corona, G. Martovetsky, B. Egan, T. Choueiri, L. Ellis, I.P. Garraway, G. M. Lee, E. Corey, H.W. Long, W. Zwart, M.L. Freedman, Prostate cancer reactivates developmental epigenomic programs during metastatic progression, Nat. Genet. 52 (2020) 790–799.
[18] R. Rubicz, S. Zhao, M. Geybels, J.L. Wright, S. Kolb, B. Klotzle, M. Bibikova, D. Troyer, R. Lance, E.A. Ostrander, Z. Feng, J.B. Fan, J.L. Stanford, DNA methylation profiles in African American prostate cancer patients in relation to disease progression, Genomics 111 (2019) 10–16.
[19] K. Daniunaite, M. Dubikaityte, P. Gibas, A. Bakavicius, J. Rimantas Lazutka, A. Ulys, F. Jankevicius, S. Jarmalaite, Clinical significance of miRNA host gene promoter methylation in prostate cancer, Hum. Mol. Genet. 26 (2017) 2451–2461.
[20] K. Chen, N. Rajewsky, The evolution of gene regulation by transcription factors and microRNAs, Nat. Rev. Genet. 8 (2007) 93–103.
[21] G.L. Gravina, F. Marampon, M. Piccolella, M. Motta, L. Ventura, R. Pomante, V.M. Popov, B.M. Zani, R.G. Pestell, V. Tombolini, E.A. Jannini, C. Festuccia, Hormonal therapy promotes hormone-resistant phenotype by increasing DNMT activity and expression in prostate cancer models, Endocrinology 152 (2011) 4550–4561.
[22] M. Chu, Y. Chang, P. Li, Y. Guo, K. Zhang, W. Gao, Androgen receptor is negatively correlated with the methylation-mediated transcriptional repression of miR-375 in human prostate cancer cells, Oncol. Rep. 31 (2014) 34–40.
[23] W. Zhou, H. Zhu, Y. Xu, L. Gu, W. Wu, Y. Zhang, X. Huang, Y. Jiang, miR-498/DNMT3b Axis mediates resistance to radiotherapy in esophageal cancer cells, Cancer Biother. Radiopharm. 37 (2022) 287–299.
[24] H. Li, Y. Lei, S. Li, F. Li, J. Lei, MicroRNA-20a-5p inhibits the autophagy and cisplatin resistance in ovarian cancer via regulating DNMT3B-mediated DNA methylation of RBP1, Reprod. Toxicol. 109 (2022) 93–100.
[25] X. Han, D. Liu, Y. Zhou, L. Wang, H. Hou, H. Chen, L. Zhang, W. Chen, X. Li, L. Zhao, The negative feedback between miR-143 and DNMT3A regulates cisplatin resistance in ovarian cancer, Cell Biol. Int. 45 (2021) 227–237.
[26] K. Ganapathy, C. Ngo, T. Andl, D. Coppola, J. Park, R. Chakrabarti, Anticancer function of microRNA-30e is mediated by negative regulation of HELLPAR, a noncoding macroRNA, and genes involved in ubiquitination and cell cycle progression in prostate cancer, Mol. Oncol. 16 (2022) 2936–2958.
[27] K. Ganapathy, S. Staklinski, M.F. Hasan, R. Ottman, T. Andl, A.E. Berglund, J.Y. Park, R. Chakrabarti, Multifaceted function of MicroRNA-299-3p fosters an antitumor environment through modulation of androgen receptor and VEGFA signaling pathways in prostate cancer, Sci. Rep. 10 (2020) 5167.

[28] R. Ottman, K. Ganapathy, H.Y. Lin, C.D. Osterman, J. Dutil, J. Matta, G. Ruiz-Deya, L. Wang, K. Yamoah, A. Berglund, R. Chakrabarti, J.Y. Park, Differential expression of miRNAs contributes to tumor aggressiveness and racial disparity in african American men with prostate cancer, Cancers 15 (2023).
[29] H. Choudhry, J.W. Catto, Epigenetic regulation of microRNA expression in cancer, Methods Mol. Biol. 676 (2011) 165–184.
[30] G. Oshima, E.C. Poli, M.J. Bolt, A. Chlenski, M. Forde, J.M.S. Jutzy, N. Biyani, M.C. Posner, S.P. Pitroda, R.R. Weichselbaum, N.N. Khodarev, DNA methylation controls metastasis-suppressive 14q32-encoded miRNAs, Cancer Res. 79 (2019) 650–662.
[31] L.C. Li, R. Dahiya, MethPrimer: designing primers for methylation PCRs, Bioinformatics 18 (2002) 1427–1431.
[32] D.F. Jarrard, H. Kinoshita, Y. Shi, C. Sandefur, D. Hoff, L.F. Meisner, C. Chang, J.G. Herman, W.B. Isaacs, N. Nassif, Methylation of the androgen receptor promoter CpG island is associated with loss of androgen receptor expression in prostate cancer cells, Cancer Res. 58 (1998) 5310–5314.
[33] H. Kim, J. Lapointe, G. Kaygusuz, D.E. Ong, C. Li, M. van de Rijn, J.D. Brooks, J.R. Pollack, The retinoic acid synthesis gene ALDH1a2 is a candidate tumor suppressor in prostate cancer, Cancer Res. 65 (2005) 8118–8124.
[34] J. Zhang, C. Yang, C. Wu, W. Cui, L. Wang, DNA methyltransferases in cancer: biology, paradox, aberrations, and targeted therapy, Cancers 12 (2020).
[35] W. Zhang, J. Xu, DNA methyltransferases and their roles in tumorigenesis, Biomark. Res. 5 (2017) 1.
[36] R. Pathania, S. Ramachandran, S. Elangovan, R. Padia, P. Yang, S. Cinghu, R. Veeranan-Karmegam, P. Arjunan, J.P. Gnana-Prakasam, F. Sadanand, L. Pei, C. S. Chang, J.H. Choi, H. Shi, S. Manicassamy, P.D. Prasad, S. Sharma, V. Ganapathy, R. Jothi, M. Thangaraju, DNMT1 is essential for mammary and cancer stem cell maintenance and tumorigenesis, Nat. Commun. 6 (2015) 6910.
[37] K.K. Wong, DNMT1: a key drug target in triple-negative breast cancer, Semin. Cancer Biol. 72 (2021) 198–213.
[38] Q. Yao, Y. Chen, X. Zhou, The roles of microRNAs in epigenetic regulation, Curr. Opin. Chem. Biol. 51 (2019) 11–17.
[39] P. Östling, S.-K. Leivonen, A. Aakula, P. Kohonen, R. Mäkelä, Z. Hagman, A. Edsjö, S. Kangaspeska, H. Edgren, D. Nicorici, A. Bjartell, Y. Ceder, M. Perälä, O. Kallioniemi, Systematic analysis of microRNAs targeting the androgen receptor in prostate cancer cells, Cancer Res. 71 (2011) 1956–1967.
[40] H. Suzuki, R. Maruyama, E. Yamamoto, M. Kai, DNA methylation and microRNA dysregulation in cancer, Mol. Oncol. 6 (2012) 567–578.
[41] M. Shiina, Y. Hashimoto, T. Kato, S. Yamamura, Y. Tanaka, S. Majid, S. Saini, S. Varahram, P. Kulkarni, P. Dasgupta, Y. Mitsui, M. Sumida, L. Tabatabai, G. Deng, D. Kumar, R. Dahiya, Differential expression of miR-34b and androgen receptor pathway regulate prostate cancer aggressiveness between African-Americans and Caucasians, Oncotarget 8 (2016) 8356–8368.
[42] M.V. Geraldo, H.I. Nakaya, E.T. Kimura, Down-regulation of 14q32-encoded miRNAs and tumor suppressor role for miR-654-3p in papillary thyroid cancer, Oncotarget 8 (2016) 9597–9607.
[43] A. Formosa, E.K. Markert, A.M. Lena, D. Italiano, E. Finazzi-Agro, A.J. Levine, S. Bernardini, A.V. Garabadgiu, G. Melino, E. Candi, MicroRNAs, miR-154, miR-299-5p, miR-376a, miR-376c, miR-377, miR-381, miR-487b, miR-485-3p, miR-495 and miR-654-3p, mapped to the 14q32.31 locus, regulate proliferation, apoptosis, migration and invasion in metastatic prostate cancer cells, Oncogene 33 (2014) 5173–5182.
[44] P.V. Jishnu, P. Jayaram, V. Shukla, V.K. Varghese, D. Pandey, K. Sharan, S. Chakrabarty, K. Satyamoorthy, S.P. Kabekkodu, Prognostic role of 14q32.31 miRNA cluster in various carcinomas: a systematic review and meta-analysis, Clin. Exp. Metastasis 37 (2020) 31–46.
[45] K.M.T. Arif, E.K. Elliott, L.M. Haupt, L.R. Griffiths, Regulatory mechanisms of epigenetic miRNA relationships in human cancer and potential as therapeutic targets, Cancers 12 (2020) 2922.
[46] E.K.O. Ng, W.P. Tsang, S.S.M. Ng, H.C. Jin, J. Yu, J.J. Li, C. Röcken, M.P.A. Ebert, T.T. Kwok, J.J.Y. Sung, MicroRNA-143 targets DNA methyltransferases 3A in colorectal cancer, Br. J. Cancer 101 (2009) 699–706.
[47] X. Wei, T. Xiang, G. Ren, C. Tan, R. Liu, X. Xu, Z. Wu, miR-101 is down-regulated by the hepatitis B virus x protein and induces aberrant DNA methylation by targeting DNA methyltransferase 3A, Cell. Signal. 25 (2013) 439–446.
[48] N. Amodio, M. Leotta, D. Bellizzi, M.T.D. Martino, P. D'Aquila, M. Lionetti, F. Fabiani, E. Leone, A.M. Gullà, G. Passarino, M. Caraglia, M. Negrini, A. Neri, A. Giordano, P. Tagliaferri, P. Tassone, DNA-demethylating and anti-tumor activity of synthetic miR-29b mimics in multiple myeloma, Oncotarget 3 (2012) 1246–1258.
[49] M. Fabbri, R. Garzon, A. Cimmino, Z. Liu, N. Zanesi, E. Callegari, S. Liu, H. Alder, S. Costinean, C. Fernandez-Cymering, S. Volinia, G. Guler, C.D. Morrison, K. K. Chan, G. Marcucci, G.A. Calin, K. Huebner, C.M. Croce, MicroRNA-29 family reverts aberrant methylation in lung cancer by targeting DNA methyltransferases 3A and 3B, Proc. Natl. Acad. Sci. U.S.A. 104 (2007) 15805–15810.
[50] R. Garzon, S. Liu, M. Fabbri, Z. Liu, C.E.A. Heaphy, E. Callegari, S. Schwind, J. Pang, J. Yu, N. Muthusamy, V. Havelange, S. Volinia, W. Blum, L.J. Rush, D. Perrotti, M. Andreeff, C.D. Bloomfield, J.C. Byrd, K. Chan, L.-C. Wu, C.M. Croce, G. Marcucci, MicroRNA-29b induces global DNA hypomethylation and tumor suppressor gene reexpression in acute myeloid leukemia by targeting directly DNMT3A and 3B and indirectly DNMT1, Blood 113 (2009) 6411–6418.
[51] Q. Xu, Y. Jiang, Y. Yin, Q. Li, J. He, Y. Jing, Y.-T. Qi, Q. Xu, W. Li, B. Lu, S.S. Peiper, B.-H. Jiang, L.-Z. Liu, A regulatory circuit of miR-148a/152 and DNMT1 in modulating cell transformation and tumor angiogenesis through IGF-IR and IRS1, J. Mol. Cell Biol. 5 (2013) 3–13.
[52] Y. Teng, X. Zuo, M. Hou, Y. Zhang, C. Li, W. Luo, X. Li, A double-negative feedback interaction between MicroRNA-29b and dnmt3a/3B contributes to ovarian cancer progression, Chem. Pharm. Bull. 39 (2016) 2341–2352.
[53] Y. Pang, J. Liu, X. Li, G. Xiao, H. Wang, G. Yang, Y. Li, S.-C. Tang, S. Qin, N. Du, H. Zhang, D. Liu, X. Sun, H. Ren, MYC and DNMT3A-mediated DNA methylation represses microRNA-200b in triple negative breast cancer, J. Cell Mol. Med. 22 (2018) 6262–6274.
[54] C. Braconi, N. Huang, T. Patel, MicroRNA-dependent regulation of DNA methyltransferase-1 and tumor suppressor gene expression by interleukin-6 in human malignant cholangiocytes, Hepatology 51 (2010) 881–890.
[55] S. Zhang, M. Pei, Z. Li, H. Li, Y. Liu, J. Li, Double-negative feedback interaction between DNA methyltransferase 3A and microRNA-145 in the Warburg effect of ovarian cancer cells, Cancer Sci. 109 (2018) 2734–2745.
[56] A.S. Azmi, Y. Li, A. Aboukameel, I. Muqbil, P.A. Philip, R.M. Mohammad, DNA-Methylation-Caused downregulation of miR-30 contributes to the high expression of XPO1 and the aggressive growth of tumors in pancreatic ductal adenocarcinoma, Cancers 11 (2019) 1101.
[57] X. Han, S. Zhen, Z. Ye, J. Lu, L. Wang, P. Li, J. Li, X. Zheng, H. Li, W. Chen, X. Li, L. Zhao, A feedback loop between miR-30a/c-5p and DNMT1 mediates cisplatin resistance in ovarian cancer cells, Chem. Pharm. Bull. 41 (2017) 973–986.
[58] V. Tzelepi, S. Logotheti, E. Efstathiou, P. Troncoso, A. Aparicio, M. Sakellakis, A. Hoang, P. Perimenis, M. Melachrinou, C. Logothetis, V. Zolota, Epigenetics and prostate cancer: defining the timing of DNA methyltransferase deregulation during prostate cancer progression, Pathology 52 (2020) 218–227.